Comparative Theoretical Study of the Electron Affinities of the Alkaline-Earth Clusters: Be_n, Mg_n, and Ca_n ($n = 2, 3$)

C. C. DÍAZ-TORREJÓN,[1,2] F. ESPINOSA-MAGAÑA,[2] ILYA G. KAPLAN[3]

[1]*Centro Nacional de Supercómputo, IPICyT, A.C., Camino a la Presa San José 2055, 78216 San Luis Potosí, SLP, México*

[2]*Centro de Investigación en Materiales Avanzados, S.C., Av. Miguel de Cervantes 120, 31109, Chihuahua, Chih., México*

[3]*Instituto de Investigaciones en Materiales, UNAM. Apdo. Postal 70–360, 04510, México D.F., México*

Received 12 May 2009; accepted 8 June 2009
Published online 19 November 2009 in Wiley Online Library (wileyonlinelibrary.com).
DOI 10.1002/qua.22387

ABSTRACT: If in atoms only one type of the electron affinity (EA) can be defined, in molecules there are three types of EAs: the vertical electron affinity (VEA), adiabatic electron affinity (AEA), and vertical electron detachment energy (VEDE). These three types of EAs for beryllium, magnesium, and calcium dimers and trimers are calculated at the all-electron MP4(SDTQ) level employing the Dunning-type basis sets. All obtained EAs satisfy the following inequality VEDE > AEA > VEA and are quite large to be observed in experiment, especially in the trimer case: VEDE (Be_3^-) = 1.63 eV, VEDE (Mg_3^-) = 0.72 eV, and VEDE (Ca_3^-) = 0.95 eV. The decomposition of VEDE into physical components (Koopmans, relaxation, and correlation) and the atomic orbital population analysis (at the NBO level) are used to elucidate the nature of the outer electron binding in studied anions.
 Int J Quantum Chem 111: 103–110, 2011

Key words: alkaline earths; electron affinities; clusters; dimmers; trimers

1. Introduction

The study of binding of an excess electron to clusters of the alkaline-earth elements is important as an instructive example of the negative cluster formation in the case of atoms not possessing the valence electrons. The alkaline-earth atoms Be, Mg, Ca, etc. in the ground state have a close outer subshell $(ns)^2$. It is quite natural that their dimers are very weakly bound only by the electron correlation forces and at the self-consistent field (SCF) level they are not stable. Thus, they can be attributed to the van der Waals molecules, as the rare-gas dimers.

The situation is changed in the alkaline-earth many-atom clusters, even in trimers. This is evidently a manifestation of many-body effects. The crucial role of the three-body forces in the stabilization of the alkaline-earth trimers and tetramers was established at the Møller–Plesset perturbation

Correspondence to: I.G. Kaplan; e-mail: kaplan@iim.unam.mx
Contract grant sponsor: DGAPA-UNAM.
Contract grant number: IN 102909.
Contract grant sponsor: CONACyT.
Contract grant number: 46770-F.

theory level up to the fourth order [MP4(SDTQ)] by Kaplan et al. [1–3].

As a result of many-body interactions, the alkaline-earth elements form solids with a quite large cohesive energy. For instance, the cohesive energy of solid Be equals 3.32 eV/atom, which is larger than that in solids of open one-valence *n*s shell atoms: Li (1.63 eV/atom) or Na (1.10 eV/atom).

It is well known that the rare-gas atoms (He, Ne, Kr, etc.) in ground state repel an additional electron, their negative ions are not stable. The same behavior takes place in the case of the alkaline-earth atoms. The Be atom binds an additional electron only in the excited state $1s^2 2s2p\ ^3P$. The experimental electron affinity, 0.291 eV [4] corresponds to the $1s^2 2s2p^2\ ^4P$ state of the Be^- anion. The theoretical calculation [5] predicted a rather close value of 0.29 eV. One may expect Be_n clusters and other alkaline-earth clusters as well to form stable anions in their ground states. As was shown in calculations of Be_n and Mg_n anion clusters at different levels of theory [6–16], it is really the case, see also the experimental measurements of the photoelectron spectra of Mg_n^- by Bowen et al. [17].

The binding energy of an attached electron (the electron affinity, EA) is equal to

$$\Delta E_e = \mathrm{EA} = E_{\mathrm{n}}(N) - E_{\mathrm{a}}(N+1) \qquad (1)$$

where N denotes a neutral system and $N + 1$ denotes an anion; n and a label the electronic states of neutral and charged systems, respectively. For molecules and clusters, depending at the internuclear distances, at which $E(N)$ and $E(N + 1)$ are calculated, three kinds of EA can be defined:

- *Vertical Electron Affinity* (VEA)—both energies in Eq. (1) are calculated at the equilibrium structure of the neutral system.
- *Adiabatic Electron Affinity* (AEA)—energies in Eq. (1) are calculated at the equilibrium structures of the neutral and charged systems, respectively.
- *Vertical Electron Detachment Energy* (VEDE)—energies in Eq. (1) are calculated at the equilibrium structure of the charged system.

In Figure 1, we represented the typical potential curves for a neutral and a stable anionic dimer. The potential curve for the stable anionic dimer is deeper than that of the neutral dimer and its equilibrium distance is usually reduced in comparison

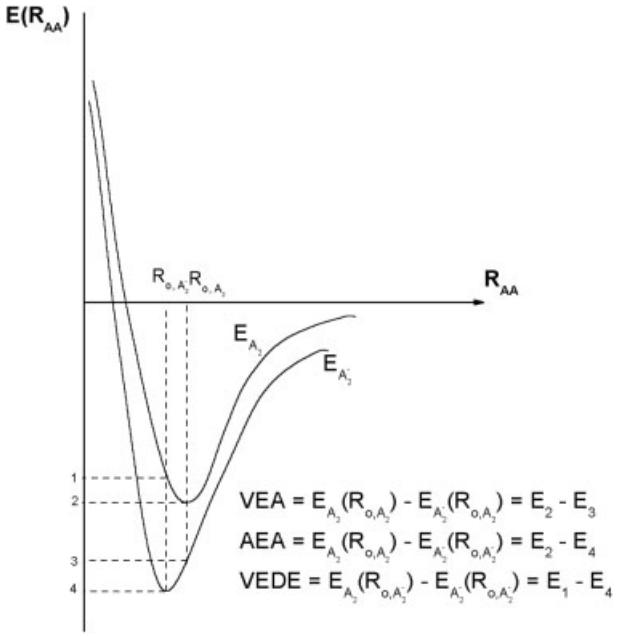

FIGURE 1. Electron affinities for a typical disposal of the potential curves of neutral and anionic dimers. 1 − $E_{A_2}(R^-_{0,A_2})$; 2 − $E_{A_2}(R_{0,A_2})$; 3 − $E^-_{A_2}(R_{0,A_2})$; 3 − $E^-_{A_2}(R^-_{0,A_2})$.

with the neutral dimer, that is, $R_0(A_2^-) < R_0(A_2)$. For this disposal of potential curves, as follows from Figure 1, the electronic affinities must satisfy the inequality:

$$\mathrm{VEDE} > \mathrm{AEA} > \mathrm{VEA} \qquad (2)$$

Theoretical studies of the electron affinities of beryllium and magnesium dimers and trimers at the MP4(SDTQ) and CCSD(T) levels were performed in Refs. [13, 14] (for beryllium the calculation were carried out up to the CCSDT level [13]). The electron affinities of the beryllium and magnesium tetramers were studied in Ref. [15] at the ROMP2 level. A reliable calculation of EAs demands the employment of large flexible basis set with diffuse functions of high angular momentum [18]. All EAs obtained in Refs. [13–15] satisfy Eq. (2) and are of the right magnitude to be observed with the standard photo-detachment technique.

In the present study, we calculated the EAs of Ca_n ($n = 2, 3$) clusters at the all-electron MP4(SDTQ) level with the Dunning-type QZ basis set [19, 20], that is, we do not use the frozen core approximation as it was in Refs. [13, 14]. To the best of our knowledge, it is the first ab initio calculation of the calcium cluster anions. For performing the compari-

TABLE I

Dependence of the ground state dimer energy (E_o) and adiabatic electron affinity (AEA) on the basis set (BS); energy calculated at the MP4(SDTQ) level.

Cluster	R_o (Å)	BS	E_o (a.u.)	AEA (eV)
Be_2	2.54	6-311 + *G*(3*d*2*f*)	−29.229312953	0.512
Be_2	2.54	*cc-pVQZ*	−29.232621398	0.420
Be_2	2.54	*aug-cc-pVQZ*	−29.232746062	0.530
Be_2^-	2.23	6-311 + *G*(3*d*2*f*)	−29.248134950	
Be_2^-	2.23	*cc-pVQZ*	−29.248060781	
Be_2^-	2.23	*aug-cc-pVQZ*	−29.252237442	
Mg_2	3.91	6-311 + *G*(3*d*2*f*)	−399.27868620	0.189
Mg_2	3.91	*cc-pVQZ*	−399.29448481	0.135
Mg_2	3.91	*aug-cc-pVQZ*	−399.29455465	0.207
Mg_2^-	3.22	6-311 + *G*(3*d*2*f*)	−399.28562728	
Mg_2^-	3.22	*cc-pVQZ*	−399.29942863	
Mg_2^-	3.22	*aug-cc-pVQZ*	−399.30216567	
Ca_2	4.40	6-311 + *G*(3*d*2*f*)	−1354.0814079	−0.407
Ca_2	4.40	*cc-pVQZ*	−1353.5757018	0.330
Ca_2^-	3.85	6-311 + *G*(3*d*2*f*)	−1354.0664496	
Ca_2^-	3.85	*cc-pVQZ*	−1353.5878280	

son with the corresponding beryllium and magnesium clusters, the latter were recalculated at the same level of accuracy. The decomposition of VEDE into three components (Koopmans, relaxation, and correlation) with clear physical sense and the atomic orbital population analysis at the NBO level are used to elucidate the nature of outer electron binding in all studied anions.

2. Methodology

All presented results were performed using the *Gaussian* 03 *Revision D*.02 suite of programs [21]. The potential energy surfaces (PES) were obtained by means of Møller–Plesset perturbation theory at MP4(SDTQ) level with all electrons involved (without the frozen-core approximation). The electron density distribution analysis was studied by the Natural Bond Orbital (NBO) analysis [22, 23] at the MP4(SDTQ) level. The ground state geometries were found varying only the interatomic distances and maintaining the symmetry in the case of trimers. For the anionic cluster, the spin contamination was monitored at the UHF and MP4 levels. To eliminate the spin contamination, the PMP4, $s + 1$, spin projection procedure [24] embedded in *Gaussian* suite, was employed.

As we noted in "Introduction" section, to describe the reliable charge distribution of an attached electron in the anionic clusters, the employed basis set (BS) in addition to standard valence basis functions must contain diffuse functions with high angular momentum. In Table I, the basis set dependence of the total energy and AEAs for neutral and anionic dimers is presented. We checked three BS: (a) 6-311+*G*(3*d*2*f*) [25], (b) *cc-pVQZ* [19, 20], and (c) *aug-cc-pVQZ* [19, 20]. BS labeled by (b) and (c) were taken directly from EMSL Basis Set Exchange web site [26–28] and (a) from *Gaussian* 03 suite. As follows from Table I, for beryllium and magnesium dimers the best results are given by *aug-cc-pVQZ* basis set, but for Ca it is not elaborated. Thus, we performed all calculations exploiting *aug-cc-pVQZ* basis set for Be and Mg clusters and *cc-pVQZ* for the Ca clusters. Let us mention that the Ca_2 anion is unstable (AEA >0) when the 6-311+*G*(3d2f) basis set is employed.

In Table II, the equilibrium distances and binding energies at ground state geometry are presented in the *frozen core* approximation and *all electrons* approach at the MP4(SDTQ) level. The inclusion of all electrons in the perturbation procedure leads to a more complete account of the electron correlation. This provides, as follows from the presented data, a more deep energy for the ground state. Especially large increase is in the Ca_2 case. It can be expected because of a large number of inner electrons in Ca_2. The all-electron MP4(SDTQ) calculations yield the equilibrium distances R_o very close to the experi-

TABLE II

Comparison of the equilibrium distance, ground state energy, and adiabatic electron affinity (AEA) of the alkaline-earth dimers calculated at the frozen core and the all-electron MP4(SDTQ) level.

	R_o (Å)			E_o (a.u.)			AEA (eV)	
Cluster	Exper.	Frozen	All	Frozen	All	ΔE_o (eV)	Frozen	All
Be_2	2.45[a]	2.54	2.46	−29.232746	−29.276523	−1.191	0.528	0.563
Mg_2	3.89[b]	3.91	3.75	−399.294555	−399.360439	−1.793	0.207	0.201
Ca_2	4.227[c]	4.40	4.24	−1353.575716	−1354.064364	−13.296	0.330	0.314

[a] Ref. [29].
[b] Refs. [29, 30].
[c] Ref. [31].

mental values for the Be_2 and Ca_2 dimers, although for Mg_2 the result is opposite. It is interesting to note that for Be_2 the all-electron AEA is larger than the frozen core one, but for the other two dimers the more account of the electron correlation decreases AEAs. The latter means that the additional electron correlation contribution in the neutral Mg and Ca dimers is larger than in their anions.

3. Results and Discussion

In Table III, we represent the equilibrium distances, ground state energies, and obtained values of three types of the electron affinities for the alkaline-earth dimers and trimers. All calculations were performed at the MP4(SDTQ) all-electron level using *aug-cc-pVQZ* BS for beryllium and magnesium clusters and *cc-pVQZ* BS for calcium clusters. The equilibrium distance for neutral dimers rises from R_0 = 2.46 Å for Be_2 to R_0 = 4.24 Å for Ca_2. The increase of the equilibrium distance in the row Be_2, Mg_2, and Ca_2 is well correlated with the increase of the average radius of atomic valence shell, which is equal 2.65 Å for Be, 3.25 Å for Mg, and 4.22 Å for Ca, see Ref. [32]. The equilibrium distances for trimers are also increased in the row Be_3, Mg_3, and Ca_3. But the addition of one more atom leads to the decrement in the equilibrium interatomic distance in comparison with dimers. The explanation of this decrement is based on the interplay of the two- and three-body interactions in the cluster formation [1].

However, EAs do not have such monotonic behavior. They decrease for Mg_n in comparison with Be_n but then increase for Ca_n, although they are still less than in the Be_n case. EAs for trimers are larger than for dimers and all EAs satisfy the condition (2),

TABLE III

Total ground state energies (E_o, a.u.) and the electron affinities (in eV) of alkaline-earths clusters calculated at the MP4(SDTQ) all-electron level.

	R_o (Å)	E_o	VEA	AEA	VEDE
Be_2	2.46	−29.276523	0.473	0.563	0.627
Be_2^-	2.20	−29.297223			
Be_3	2.19	−43.958333	1.522	1.576	1.629
Be_3^-	2.09	−44.016253			
Mg_2	3.75	−399.360439	0.095	0.201	0.271
Mg_2^-	3.19	−399.367840			
Mg_3	3.29	−599.052466	0.693	0.718	0.722
Mg_3^-	3.18	−599.078698			
Ca_2	4.24	−1354.064364	0.313	0.314	0.390
Ca_2^-	3.73	−1354.075917			
Ca_3	3.87	−2031.118088	0.885	0.919	0.951
Ca_3^-	3.71	−2031.151858			

VEDE is the largest among the three calculated affinities.

All values of EAs are quite large for being observed in experiment, especially for trimers: VEDE (Be_3^-) = 1.629 eV, VEDE (Mg_3^-) = 0.722 eV, and VEDE (Ca_3^-) = 0.951 eV. As was demonstrating in Ref. [13], where AEs for beryllium clusters were calculated at three levels of theory: MP4(SDTQ), CCSD(T), and CCSDT, the MP4(SDTQ) calculations slightly overestimate the EA's, whereas the CCSD(T) approximation underestimates the values of EA's. Thus, we may expect that the reliable values of EAs should be less than that represented in Table III.

For study of the nature of the excess electron binding in anions, it is useful to decompose its binding energy (EA) into tree components

$$\Delta E_e = \mathrm{EA} = \Delta E_e^{\mathrm{KT}} + \Delta E_{\mathrm{relax}}^{\mathrm{SCF}} + \Delta E_e^{\mathrm{corr}}. \qquad (3)$$

The Koopmans approach corresponds to the SCF method, in which both energies in Eq. (1) are calculated with the same SCF orbitals. According to the Koopmans theorem (KT)[33], the difference between the HF energies is equal to the negative of the relevant orbital energy. For the VEDE the Koopmans contribution is determined at the anion equilibrium geometry as

$$\Delta E_e^{\mathrm{KT}}(\mathrm{VEDE}) = E_0^{\mathrm{SCF}}(N) - E_0^{\mathrm{SCF}}(N+1)_{\text{non-relax}} = -\varepsilon_e(A_n) \qquad (4)$$

where $\varepsilon_e(A_n)$ is the energy of the vacant orbital in the neutral system at its ground state occupied by the attached electron in an anion. The KT approximation does not take the relaxation effects into account and includes only the electrostatic and exchange interactions at the first order of the perturbation theory (it corresponds to the Heitler-London approximation). The remainder of the binding energy at the SCF level, we denote as the relaxation energy

$$\Delta E_{\mathrm{relax}}^{\mathrm{SCF}} = \Delta E_e^{\mathrm{SCF}} - \Delta E_e^{\mathrm{KT}}, \qquad (5)$$

which stems from the relaxation of the orbitals of the neutral system in the field of the attached electron. $\Delta E_{\mathrm{relax}}^{\mathrm{SCF}}$ consists mostly of the induction (polarization) energy, but contains also the exchange energy that cannot be separated from the induction energy.

TABLE IV

Decomposition of VEDE (in eV) in the ground states of Be, Mg, and Ca anions at the MP4(SDTQ) all-electron level.

	ΔE_e^{KT}	$\Delta E_{\mathrm{relax}}^{\mathrm{SCF}}$	$\Delta E_e^{\mathrm{corr}}$	VEDE
Be_2^-	−0.054	0.228	0.453	0.627
Be_3^-	0.148	0.581	0.900	1.629
Mg_2^-	−0.210	0.315	0.166	0.271
Mg_3^-	−0.014	0.288	0.448	0.722
Ca_2^-	−0.141	0.438	0.101	0.390
Ca_3^-	0.052	0.526	0.373	0.951

The electron correlation contribution is defined following the general definition of Lőwdin [34]

$$\Delta E_e^{\mathrm{corr}} = \Delta E_e - \Delta E_e^{\mathrm{SCF}} \qquad (6)$$

and depends on the correlation method used. In our calculation the MP4(SDTQ) method is employed, so

$$\Delta E_e^{\mathrm{corr}}(\mathrm{MP4(SDTQ)}) = \Delta E_e^{\mathrm{MP4(SDTQ)}} - \Delta E_e^{\mathrm{SCF}}. \qquad (7)$$

At large distances where the exchange effects are negligible, the correlation contribution to the binding energy reduces to the dispersion energy, as was demonstrating in the calculation of the alkaline-earth dimers in Ref. [2]. The relaxation energy at large distances reduces to the classical induction energy.

In Table IV, the decomposition (3) of VEDE at the MP4(SDTQ) level for the alkaline-earth anions is represented using Eqs. (4)–(7). Let us discuss the conclusions according the binding of the excess electron, separately for dimers and trimers.

3.1. DIMERS

For all anionic dimers, the Koopmans contribution, which includes the electrostatic and exchange interactions, is negative; so it plays a destabilizing role. On the other hand, the relaxation energy, which includes induction and exchange energies, is large enough to stabilize these anions at the SCF level. The anionic dimers are stabilized by the relaxation and correlation energies. The main contribution for Be_2^- and Mg_2^- comes from the correlation energy, while in the Ca_2^- case the relaxation energy contributes more.

TABLE V

Atomic orbital population $n_l(A)$ in neutral and anionic alkaline earths, obtained by the natural bond orbitals (NBO) analysis at the MP4(SDTQ) all-electron level, and the atomic orbital distribution of the excess electron Δe_l, Eq. (8).

	2s	2p	3s	3p	3d	4s	4p	4d	4f	5s
Be_2	1.95	0.04	—	—	—	0.01	—	—	—	—
Be_2^-	1.90	0.57	—	0.01	0.02	—	—	—	—	—
Δe_l(Be)	−0.05	0.53	—	0.01	0.02	−0.01	—	—	—	—
Be_3	1.72	0.26	—	0.01	—	—	—	—	—	—
Be_3^-	1.74	0.55	—	0.01	0.02	—	—	—	0.01	—
Δe_l(Be)	0.02	0.29	—	0.00	0.02	—	—	—	0.01	—
Mg_2	—	—	1.99	—	—	—	0.01	—	—	—
Mg_2^-	—	—	1.97	0.51	0.01	—	—	—	—	—
Δe_l(Mg)	—	—	−0.02	0.51	0.01	—	−0.01	—	—	—
Mg_3	—	—	1.95	0.04	—	—	—	—	—	—
Mg_3^-	—	—	1.92	0.37	0.03	—	—	—	0.01	—
Δe_l(Mg)	—	—	−0.03	0.33	0.03	—	—	—	0.01	—
Ca_2	—	—	—	—	—	1.98	0.01	—	—	—
Ca_2^-	—	—	—	—	0.11	1.90	0.49	—	—	—
Δe_l(Ca)	—	—	—	—	0.11	−0.08	0.48	—	—	—
Ca_3	—	—	—	—	—	1.90	0.08	0.01	—	0.01
Ca_3^-	—	—	—	—	0.10	1.90	0.32	—	—	—
Δe_l(Ca)	—	—	—	—	0.10	0.00	0.24	−0.01	—	−0.01

3.2. TRIMERS

All anionic trimers are stable at the SCF level. The main contribution to the Be_3^- and Mg_3^- stability yields the correlation energy, while, as for the calcium dimer, for Ca_3^- the contribution of the relaxation energy is larger. At large distances the relaxation and dispersion terms reduce to the induction and dispersion energies, respectively, between the excess electron and the neutral trimers, but at distances in anions they cannot be separated from the exchange and overlap effects [35].

It is important to mention that three-atomic clusters, especially anions, can undergo the Jahn–Teller distortion [36] and not be stable at the considered equilateral triangular geometry (the point symmetry group D_{3h}). As follows from our calculations for all studied anion trimers the ground state belongs to the one-dimensional representation, A_2''. The outmost electron occupied orbital with the symmetry A_2'' (see Figs. 3, 5). Thus, the anionic trimers can be studied at the adiabatic approximation without taking into account the Jahn–Teller effect. On the other hand, we may not exclude the pseudo Jahn–Teller effect, the second-order Jahn–Teller distortions, which can lead to transformation of the equilateral triangle into the isosceles triangle. But this is a subject for a separate vibronic calculation and is beyond the scope of our study.

It is instructive to study the atomic orbital population in anions and compare it with the atomic orbital population in neutral clusters. We studied it by the Natural Bond Orbital (NBO) analysis that is more precise than the Mulliken population analysis. In Table V, we represented the atomic orbital population for neutral and anionic alkaline-earth dimers and trimers. It is useful to mention that the atomic orbital population in the neutral alkaline-earth dimers and trimers is discussed in details in Refs. [2, 3]. As follows from these studies, while in the isolated atoms at the SCF approximation only the *n*s subshell is populated (it is closed, $(ns)^2$), the correlation effects and interatomic interactions induce the population of *n*p shell This gives rise to the sp-hybridization in the alkaline-earth clusters. In our study, we are interested in the nature of the anion stabilization. Therefore, it is important to study the distribution of the excess electron among the atomic states. It is described as the difference between the anionic and neutral atomic orbital populations

$$\Delta e_l(A) = n_l(A_n^-) - n_l(A_n) \tag{8}$$

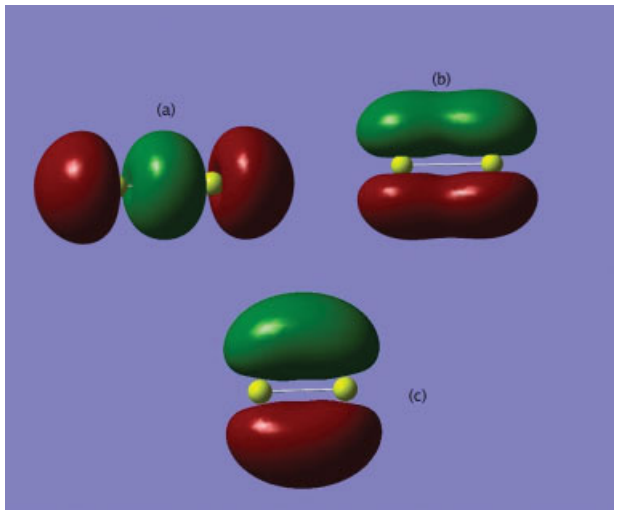

FIGURE 2. Molecular orbital diagrams in the magnesium dimer: (a) Mg_2 LUMO, (b) Mg_2 LUMO +1, (c) Mg_2^- HOMO, symmetry σ_u. [Color figure can be viewed in the online issue, which is available at wileyonlinelibrary.com.]

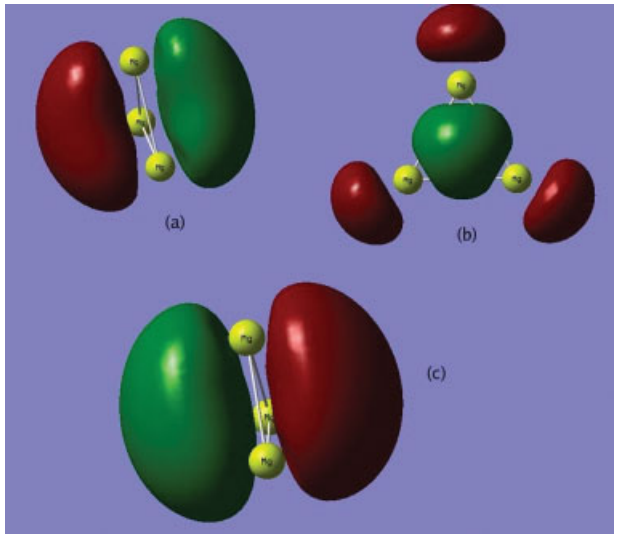

FIGURE 3. Molecular orbitals in the magnesium trimer: (a) Mg_3 LUMO, (b) Mg_3 LUMO +1, (c) Mg_3^- HOMO, symmetry A_2''. [Color figure can be viewed in the online issue, which is available at wileyonlinelibrary.com.]

This difference is presented in Table V for all studied clusters.

The excess electron is equally distributed among atoms. Multiplying the values of $\Delta_l(A)$ in Table V by 2 for dimers and 3 for trimers, we obtain the orbital population of the outer electron in anions A_n^- (the negative population of some orbitals means that the population of these orbitals in anion is less than it is in the neutral cluster):

$$\begin{cases} \Delta e_l(\mathrm{Be}_2^-)\text{: } 2s^{-0.1}2p^{1.06}3p^{0.02}3d^{0.04}4s^{-0.02} \\ \Delta e_l(\mathrm{Be}_3^-)\text{: } 2s^{0.06}2p^{0.87}3d^{0.06}4f^{0.03} \\ \Delta e_l(\mathrm{Mg}_2^-)\text{: } 3s^{-0.04}3p^{1.02}3d^{0.02}4p^{-0.02} \\ \Delta e_l(Mg_3^-)\text{: } 3s^{-0.09}3p^{0.99}3d^{0.09}4f^{0.03} \\ \Delta e_1(\mathrm{Ca}_2^-)\text{: } 3d^{0.22}4s^{-0.16}4p^{0.96} \\ \Delta e_l(Ca_3^-)\text{: } 3d^{0.30}4p^{0.72}4d^{-0.03}5s^{-0.03} \end{cases} \quad (9)$$

Thus, in the beryllium and magnesium anions the attached electron mostly occupies the p-type orbitals. In calcium anions it is distributed among 4p-orbitals and 3d-orbitals. In Ca_3^-, the population of 3d-orbital is quite large, 0.3 *e*.

The alkaline-earth anions are evidently may be considered as valence-bound and the excess electron must occupy one of the valence vacant orbitals in the neutral cluster. In Figs. 2–5, we represented plots of two lowest unoccupied molecular orbitals (LUMO and LUMO + 1) in neutral clusters and highest occupied molecular orbitals in corresponding anions. From the symmetry of the orbitals it follows that for magnesium and calcium dimers the outer electron in anions occupies LUMO + 1 orbital, while in trimers it occupies LUMO.

As follows from the orbital population analysis and presented molecular orbital diagrams (Figs. 2–5), the studied anions must be attributed to the valence-bound anions.

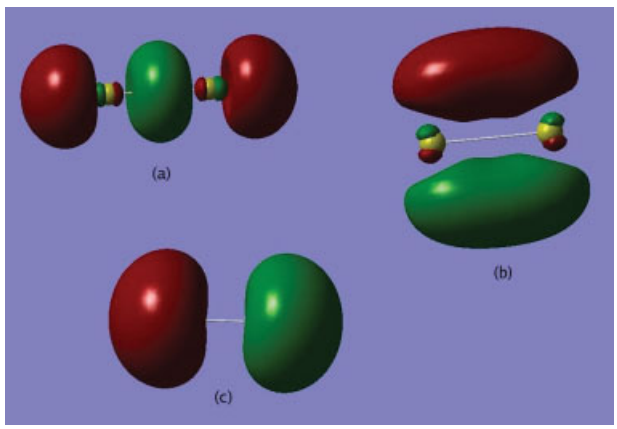

FIGURE 4. Molecular orbitals in the calcium dimer: (a) Ca_2 LUMO, (b) Ca_2 LUMO +1, (c) Ca_2^- HOMO, symmetry π_u. [Color figure can be viewed in the online issue, which is available at wileyonlinelibrary.com.]

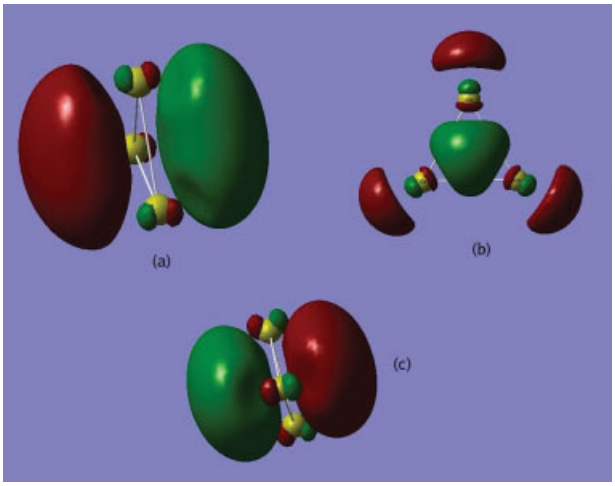

FIGURE 5. Molecular orbitals in the calcium trimer: (a) Ca_3 LUMO, (b) Ca_3 LUMO +1, (c) Ca_3^- HOMO, symmetry A_2''. [Color figure can be viewed in the online issue, which is available at wileyonlinelibrary.com.]

ACKNOWLEDGMENTS

We are grateful to Victor Polinger and a referee of our article for useful comments. The authors would like to acknowledge the National Supercomputer Center (CNS) of IPICyT, A.C. for supercomputer facilities.

References

1. Kaplan, I. G.; Hernández-Cobos, J.; Ortega-Blake, I.; Novaro, O. Phys Rev A 1996, 53, 2493.
2. Kaplan, I. G.; Roszak, S.; Leszczinski, J. J Chem Phys 2000, 113, 6245.
3. Kaplan, I. G.; Roszak, S.; Leszczinski, J. Adv Quantum Chem 2001, 40, 257.
4. Kristensen, P.; Petrunin, V. V.; Andersen, H. H.; Andersen, T. Phys Rev A 1995, 52, R2508.
5. Hsu, J. J.; Chung, K. T. Phys Rev A 1995, 52, R898.
6. Jordan, K. D.; Simons, J. J Chem Phys 1977, 67, 4027.
7. Jordan, K. D.; Simons, J. J Chem Phys 1980, 72, 2889.
8. Jordan, K. D.; Simons, J. J Chem Phys 1982, 77, 5250.
9. Bauschlicher, C. W., Jr.; Patridge, H. J Chem Phys 1984, 80, 334.
10. (a) Reuse, F.; Khanna, S. N.; de Coulon, V.; Buttet, J. Phys Rev B 1989, 39, 12911; (b) Reuse, F.; Khanna, S. N.; de Coulon, V.; Buttet, J. Phys Rev B 1990, 41, 11743.
11. Acioli, P. H.; Jellinek, J. Phys Rev Lett 2002, 89, 213402.
12. Jellinek, J.; Acioli, P. H. J Phys Chem A 2002, 106, 10919.
13. Kaplan, I. G.; Dolgounitcheva, O.; Watts, J. D.; Ortiz, J. V. J Chem Phys 2002, 117, 3687.
14. Kaplan, I. G.; Díaz, C. C. Int J Quantum Chem 2005, 104, 468.
15. Díaz, C. C.; Kaplan, I. G.; Roszak, S. J Mol Model 2005, 11, 330.
16. Zhang, J. M.; Duan, Y. N.; Xu, K. W.; Ji, V.; Man, Z. Y. Physica B 2008, 403, 3119.
17. Thomas, O. C.; Zeng, W.; Xu, S.; Shiloh, M.; Bowen, K. H. Phys Rev Lett 2002, 89, 213403.
18. Dunning, T. H., Jr.; Peterson, K. A.; van Mourik, T. In Calculations of Electronic Affinities. A Roadmap in Dissociative Recombination of Molecular Ions with Electrons; Guberman, S. L., Eds.; Kluver Academic Press: New York, 2003; p 415.
19. Woon, D. E.; Dunning, T. H., Jr. J Chem Phys 1993, 98, 1358.
20. Woon, D. E.; Dunning, T. H., Jr. J Chem Phys 1995, 103, 4572.
21. Gaussian 03, Revision D. 02, Frisch, M. J.; Trucks, G. W.; Schlegel, H. B.; Scuseria, G. E.; Robb, M. A.; Cheeseman, J. R.; Montgomery, J. A., Jr.; Vreven, T.; Kudin, K. N.; Burant, J. C.; Millam, J. M.; Iyengar, S. S.; Tomasi, J.; Barone, V.; Mennucci, B.; Cossi, M.; Scalmani, G.; Rega, N.; Petersson, G. A.; Nakatsuji, H.; Hada, M.; Ehara, M.; Toyota, K. Fukuda, R.; Hasegawa, J.; Ishida, M.; Nakajima, T.; Honda, Y.; Kitao, O.; Nakai, H.; Klene, M.; Li, X.; Knox, J. E.; Hratchian, H. P.; Cross, J. B.; Bakken, V.; Adamo, C.; Jaramillo, J.; Gomperts, R.; Stratmann, R. E.; Yazyev, O.; Austin, A. J.; Cammi, R.; Pomelli, C.; Ochterski, J. W.; Ayala, P. Y.; Morokuma, K.; Voth, G. A.; Salvador, P.; Dannenberg, J. J.; Zakrzewski, V. G.; Dapprich, S.; Daniels, A. D.; Strain, M. C.; Farkas, O.; Malick, D. K.; Rabuck, A. D.; Raghavachari, K.; Foresman, J. B.; Ortiz, J. V.; Cui, Q.; Baboul, A. G.; Clifford, S. Cioslowski, J.; Stefanov, B. B.; Liu, G.; Liashenko, A.; Piskorz, P.; Komaromi, I.; Martin, R. L.; Fox, D. J.; Keith, T.; Al-Laham, M. A.; Peng, C. Y.; Nanayakkara, A.; Challacombe, M.; Gill, P. M. W.; Johnson, B.; Chen, W.; Wong, M. W.; Gonzalez, C.; Pople, J. A. Gaussian, Inc., Wallingford CT, 2004.
22. Biegler-König, F. W.; Bader, R. F. W.; Tang, T. H. J Comput Chem 1982, 3, 317.
23. Wiberg, K. B.; Hadad, C. M.; LePage, T. J.; Breneman, C. M.; Frisch, M. J. J Phys Chem 1992, 96, 671.
24. Schlegel, H. B. J Chem Phys 1986, 84, 4530.
25. Frisch, M. J.; Pople, J. A.; Binkley, J. S. J Chem Phys 1984, 80, 3265.
26. EMSL web site. Available at: https://bse.pnl.gov/bse/portal. Accessed on August 24, 2008.
27. Feller, D. J. J Comput Chem 1996, 17, 1571.
28. Schuchardt, K. L.; Didier, B. T.; Elsethagen, T.; Sun, L.; Gurumoorthi, V.; Chase, J.; Li, J.; Windus, T. L. J Chem Inf Model 2007, 47, 1045. Doi:10.1021/ci600510j.
29. Bondybey, E. Chem Phys Lett 1984, 109, 436.
30. Balfour, W. J.; Douglas, A. E. Can J Phys 1970, 48, 901.
31. Vidal, C. R. J Chem Phys 1980, 72, 1864.
32. Bunge, C. F.; Barrientos, J. A.; Vivier-Bunge, A. At Data Nucl Data Tables 1993, 53, 113.
33. Koopmans, T. Physica (Amsterdam) 1934, 1, 104.
34. Lőwdin, P. O. Adv Chem Phys 1959, 2, 207.
35. Kaplan, I. G. Intermolecular Interactions: Physical Pictures Computational Methods, and Model Potentials; Wiley: Chichester, 2006.
36. Bersuker, I. B. The Jahn-Teller Effect; Cambridge University Press: Cambridge, 2006.